Journal of Structural Biology 170 (2010) 152–156

Contents lists available at ScienceDirect

Journal of Structural Biology

journal homepage: www.elsevier.com/locate/yjsbi

Graphene oxide: A substrate for optimizing preparations of frozen-hydrated samples

Radosav S. Pantelic [a], Jannik C. Meyer [b], Ute Kaiser [b], Wolfgang Baumeister [a], Jürgen M. Plitzko [a,*]

[a] Max Planck Institute of Biochemistry, Department of Molecular Structural Biology, Martinsried, Germany
[b] University of Ulm, Electron Microscopy Department of Materials Sciences, Ulm, Germany

ARTICLE INFO

Article history:
Received 23 October 2009
Received in revised form 15 December 2009
Accepted 18 December 2009
Available online 24 December 2009

Keywords:
Graphene
Graphene oxide
Cryo-EM
Electron microscopy

ABSTRACT

Graphene oxide is a hydrophilic derivative of graphene to which biological macromolecules readily attach, with properties superior to those of amorphous carbon films commonly used in electron microscopy. The single-layered crystalline lattice of carbon is highly electron transparent, and exhibits conductivity higher than amorphous carbon. Hence, graphene oxide is a particularly promising substrate for the examination of biological materials by electron microscopy. In this manuscript we compare graphene oxide films to commonly used amorphous carbon films, describing the use of graphene in optimizing the preparation of unstained, vitrified biological macromolecules.

1. Introduction

Films made of evaporated carbon are routinely used as substrates for the mounting and subsequent imaging of biological samples by electron microscopy. When imaged at higher magnifications such amorphous carbon substrates display a granular texture, attenuating and even obscuring the signal of unstained particles. Hence, to circumvent this limitation frozen-hydrated samples are often imaged within unsupported regions of vitreous ice prepared across perforated carbon films. However, a problem sometimes encountered with such preparations is the tendency of biological macromolecules to adsorb strongly to the surrounding carbon leading to a depletion of particles within the spanning vitreous ice. This in particular, is an issue with preparations that require washing to remove unwanted low molecular weight constituents, as most of the sample is also subsequently removed.

Graphene is a single-layer crystalline lattice of sp^2 bound carbon atoms (Geim and Novoselov, 2007) possessing several advantages over amorphous carbon. The ideal (i.e. uncontaminated and defect free) graphene structure is expected to be essentially featureless down to a resolution of 2.13 Å. If sampled at higher resolution, the regular crystallinity of graphene gives rise to a periodic signal that can be subtracted if necessary (Meyer et al., 2008). The single-layer thickness (0.34 nm, Eda et al., 2008) of graphene also minimizes electron scattering within the substrate and hence any background noise. The conductivity of pristine graphene, converted to bulk units assuming a thickness of 3.4 Å, is more than six orders of magnitude higher than the conductivity of amorphous carbon (Chen et al., 2008; Robertson, 1986; Ziegler, 2006). Therefore, graphene may reduce charging effects and improve the imaging stability of insulating materials like amorphous ice. Graphene reacts to deformation elastically (Lee et al., 2008; Zakharchenko et al., 2009) and has a high mechanical strength (Wang et al., 2009), allowing it to withstand sonication as well as other harsh (chemical) treatments (Reina et al., 2009).

Although hydrophobic, graphene can be functionalized using chemical processes (Wang et al., 2009; Schniepp et al., 2006), thereby producing hydrophilic substrates to which molecules readily attach. Graphene oxide is one such derivative produced by the exfoliation of graphite oxide, a heavily oxygenated and hydrophilic form of graphite (Paredes et al., 2008; Wei et al., 2008). Fig. 1 shows an area of 1–2 layer thin graphene oxide substrate. Although oxidization attenuates the material properties of pristine graphene (see Section 4), substrates are stable and demonstrate significantly reduced background contrast. Clearly defined hexagonal diffraction patterns (Fig. 1, insets A and B) occurring at the material periodicities (2.13 and 1.23 Å, respectively, Meyer et al., 2007) correspond to disordered stacking of individual graphene oxide layers.

When preparing difficult and fragile samples, sometimes also requiring multiple washes prior to vitrification, the use of additional amorphous carbon substrate is routine. In this manuscript we compare graphene oxide to amorphous carbon and describe its use as a supporting substrate for unstained, frozen-hydrated samples.

* Corresponding author. Fax: +49 8985782641.
E-mail address: plitzko@biochem.mpg.de (J.M. Plitzko).

1047-8477/$ - see front matter © 2009 Elsevier Inc. All rights reserved.
doi:10.1016/j.jsb.2009.12.020

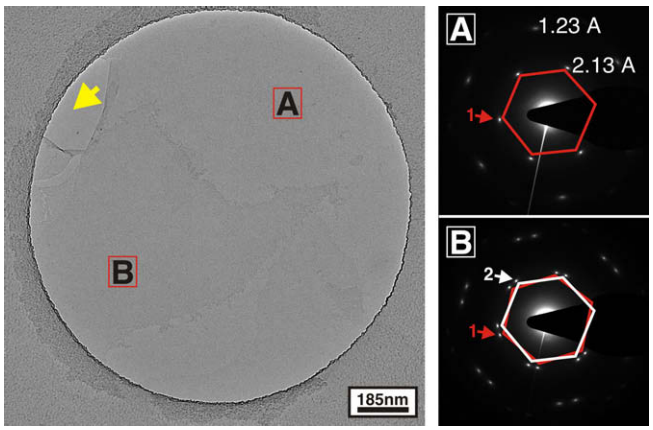

Fig. 1. Graphene oxide substrate: An area of 1 μm CFLAT spanned by single (A) and double (B) layers of graphene oxide (magnification 9400×, defocus −2 μm, pixel size 7.4 Å). Corresponding diffraction patterns (panels A and B, respectively, D 300 mm) show the periodicities of the material at 2.13 and 1.23 Å. Multiple, superimposed hexagonal patterns correspond to the unordered stacking of multiple layers. Note the minimal contrast of the few-layer region in comparison to vacuum as can be seen from a tear in the graphene oxide substrate (arrow).

2. Methods

2.1. Graphene oxide

Graphite oxide is produced according to the Hummers method (Hummers and Offeman, 1958) in which graphite mixed with concentrated sulfuric acid is exposed to strong oxidizing agents such as sodium nitrate, potassium permanganate and hydrogen peroxide during a controlled reaction. In this experiment highly ordered pyrolytic graphite (HOPG) with a 150 μm grain size (Sigma, Munich, Germany) was used. However, we have also successfully oxidized natural graphite with grain sizes of 500–1800 μm (NGS Naturgraphit GmbH, Leinburg, Germany), finding that the large flakes tend to produce larger graphene sheets.

Graphite oxide solution at ~1.5 mg/ml concentration was prepared by adding the oxidized graphite to Ω-filtered water with a pH of 7 (at pH 6.75–8.5 graphene readily attaches to substrates (Wei et al., 2008). The graphite oxide solution was then exfoliated into *graphene* oxide by sonication at 35 kHz for 30–60 min using a standard bath sonicator operated at room temperature. Following exfoliation of the graphene oxide, the suspension was left standing overnight allowing heavy particulates including thicker graphene/graphite platelets to sediment (Paredes et al., 2008). We find this often sufficient with lower graphene concentrations, although brief low speed centrifugation (~980 to 6000*g*) is sometimes also useful.

When preparing graphene oxide from coarser natural graphite flakes (500–1800 μm), the largely intact graphite pieces lead to inhomogeneous concentrations of *graphite* oxide in solution and consequently diminished exfoliation. Hence, an additional 'pre-exfoliation' of the coarser *graphite* oxide using a probe sonicator is required to ensure sufficiently homogenous concentration prior to final exfoliation of the graphene. Using 1800 μm graphite flakes, we have found that probe sonication (Branson Sonifier 250, Danbury, USA, operated with a tip intensity of 5 and 100% duty cycle) for ~5 min ensures sufficient homogeneity by dispersing the large flakes in solution.

Exfoliation is a largely uncontrolled process and therefore final concentrations are somewhat variable. Graphene oxide solution has an absorption peak at ~230 nm, and so UV–vis absorption spectra can be used to survey concentration (Paredes et al., 2008). Suitable graphene oxide coatings were obtained using exfoliated preparations with an optical density/absorption of ~2 at 230 nm (10 mm path length). Very high concentrations lead to the accumulation of folded layers and thicker coatings over the grid, in which case it is best to lower concentration by centrifugation (as previously mentioned). The exfoliated graphene oxide sheets self-adhere over time (Wei et al., 2008) and as we have found, consequently crumple and conglomerate. Therefore, the exfoliated graphene oxide solutions have a limited shelf life (~2–3 weeks) within which optimal results for this application can be expected.

2.2. Coating preparation

Grids are prepared as needed to minimize adhesion of amorphous contaminants to the strongly hydrophilic surface of the graphene oxide. Quantifoil (Quantifoil Micro Tools GmbH, Jena, Germany, 1.2/1.3 μm) and CFLAT (Protochips Inc., Raleigh, USA, 1/1 μm) EM grids were plasma cleaned with H_2 and O_2 (at gas flows of 6.4 sccm and 27.5 sccm, respectively) using a Gatan Solarus model 950, plasma cleaner for 10 s (Gatan Inc., Pleasanton, USA). A ~1 μm hole size is suitable as it ensures sufficient stability and coverage by the graphene oxide substrate. A 4 μl drop of exfoliated graphene oxide solution was applied to the glow discharged side and left to settle for ~1 min during which electrostatic interaction guides graphene sheets to the perforated carbon substrate (Wei et al., 2008) where they are strongly held in place by van der Waals forces (Reina et al., 2009; Meyer et al., 2008). By careful blotting most of the solution is removed before drying at room temperature under constant flow of nitrogen gas in order to minimize contamination.

Prior to use, the graphene oxide substrate may be partially reduced by baking for ~3 to 5 min (up to 300 °C in air, placing grids graphene side up on a standard heating plate), subsequently removing amorphous material from the crystalline substrate and optimizing the attenuated graphene properties. At 100 °C the substrate undergoes ~15% mass loss as adsorbed water is removed (Paredes et al., 2008). The highest loss of ~30% occurs at 200 °C as labile oxygen groups are removed, and up to a further 20% in *excess* of 300 °C as more stable functional groups are slowly and gradually removed (Paredes et al., 2008; Zhang et al., 2009).

2.3. Vitrified samples

Vitrified samples were prepared with a 26S proteasome sample from *Drosophila melanogaster*, as described previously (Nickell et al., 2007). From a nominal concentration of ~0.2 mg/ml, the 26S sample was further diluted with buffer (50 mM Tris/HCl, pH 7.5, 5 mM $MgCl_2$, 1 mM DTT, 2 mM ATP) to a final concentration of ~0.1 mg/ml (approximately half of that we have used when preparing conventional vitrified samples in the absence of additional substrate). With no glow discharging, 4 μl of sample was applied to graphene oxide coated Quantifoil grids and left to incubate for ~2 min before washing thrice (with the aforementioned dilution buffer to avoid depletion of ATP). Using an FEI Vitrobot Mark IV, grids were blotted for 3 s at 10 °C and 100% humidity before plunging them into liquid ethane.

The 20S proteasome from *Thermoplasma acidophilum* was prepared according to the previously published protocol (Zwickl et al., 1992). The initial sample concentration of 3 mg/ml was diluted to a final concentration of ~0.125 mg/ml, and a 3 μl drop applied to a freshly coated Quantifoil (no glow discharge). The sample was left to incubate for ~1 min before washing twice with water. Using the Vitrobot, excess buffer was blotted exhaustively leaving only strongly bound water (7 s, 10 °C and 100% humidity), then plunged into liquid ethane to prevent complete dehydration.

2.4. Imaging

A comparison of power spectra from graphene oxide and amorphous carbon (Fig. 2) was carried out using an FEI Titan 80–300 low base TEM equipped with image spherical aberration corrector (spherical aberration C_s = 0, ±2 μm) operated at 80 keV. Thin amorphous carbon and graphene oxide samples were imaged at 145,000× magnification (unbinned pixel size 0.87 Å) and ~200 nm defocus to CCD (1 s exposure time, Gatan US1000, 1024 × 1024 pixel, 24 μm physical pixel size). Diffraction patterns were collected with a 10 μm SA aperture, 245 mm camera length and 1 s exposure time.

Vitreous and unstained samples (Figs. 3 and 4) were imaged at liquid nitrogen temperature with an FEI Titan KRIOS high-base system (equipped with Autoloader) operated at 300 keV. Data were recorded with a TVIPS 8192 × 8192 pixel (15.8 μm physical pixel size; TVIPS GmbH, Gauting, Germany) CCD/CMOS camera at 0.5 s exposure time. Overview images of vitrified 26S and 20S proteasomes were taken at a calculated magnification of 88,500× and 2× binning yielding a final pixel size of 3.5 Å.

3. Results

3.1. Background signal comparison

Fig. 2 compares calculated power spectra from separate single-layer (see inset) graphene oxide (Fig. 2, green, ~300 °C baked) and thin amorphous carbon (Fig. 2, black, ~3–4 nm thick) samples, imaged at 145 k× magnification and ~200 nm defocus. According to a widely accepted model (Lerf et al., 1998), graphene oxide consists of defect-free crystalline areas (Fig. 3A) interspersed with clustered oxidized regions (Fig. 3B) to which the sample molecules attach. These functional groups form irregularities on a nanometer scale that contribute to the limited scattering of the substrate.

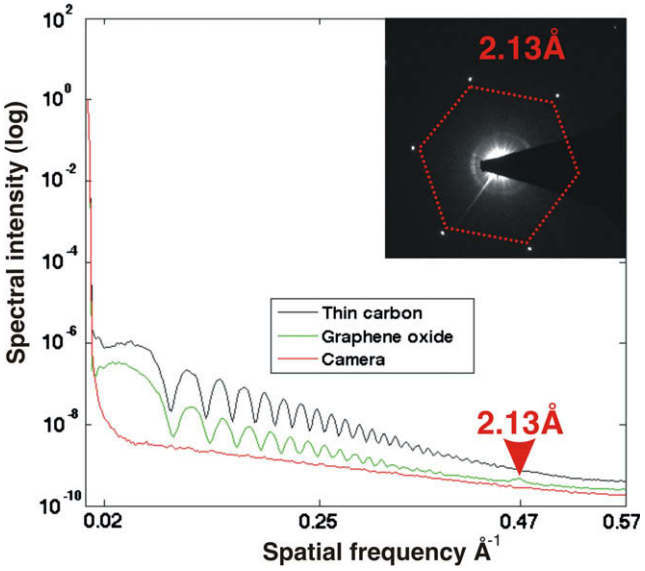

Fig. 2. Comparison of amorphous carbon and graphene background signal: The power spectra of separately prepared graphene oxide (green) and thin amorphous carbon (black, ~3 to 4 nm thick) regions (magnification 145 k×, 0.87 Å pixel size, ~200 nm defocus) are compared. Images have been normalized according to their mean pixel value prior to calculation. The inset shows diffraction (D 245 mm) of the graphene oxide substrate, a singular hexagonal pattern indicating an individual layer. Minimized scattering is contributed by attached functional groups. However, graphene oxide demonstrates clear benefit in terms of reduced substrate signal and significantly reduced background (seen by the shift in baseline, note log scaling) close to that of the CCD camera alone (red).

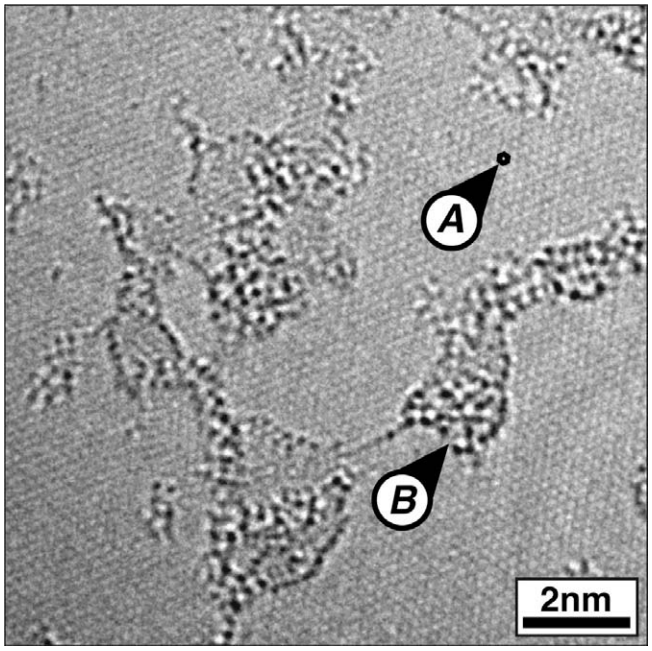

Fig. 3. Atomic image of graphene oxide: An area of graphene oxide (380 k× magnification, 0.26 Å pixel size, 9 nm defocus, imaged from the same grid used in Fig. 2) showing the largely crystalline proportion of the substrate (A, note hexagonal pitch of carbon atoms as indicated) interspersed with clustered functional groups (B) contributed by the materials oxidization. This functionalization yields limited scattering but also contributes the substrates hydrophilic properties suited to attaching biological molecules.

Comparing graphene oxide to thin amorphous carbon, there is a difference in both background signal (baseline) and modulation amplitude of ~40% (note log scaling), as well as rapid tapering of the modulation envelope up to 0.35 $Å^{-1}$ (as opposed 0.42 $Å^{-1}$). The modulation (Thon rings) corresponds to oscillations of the phase contrast transfer function (pctf), therefore indicating the differences in the elastic, phase contrast contributions of the different support films. Importantly, there is also a significant background signal from the amorphous carbon film that is not modulated by the pctf, and likely attributed to amplitude contrast from multiple and inelastic scattering by the substrate. The minimized scattering cross-section of the much thinner, non-amorphous graphene oxide substrate yields significantly reduced background signal, and is particularly impressive compared to the background signal (noise) contributed by the CCD alone (Fig. 2, red, obtained by illuminating the CCD under the same conditions with no sample). A small peak in the power spectrum of the graphene oxide (as marked at 2.13 Å) corresponds to the first periodicity of the material (seen in the diffraction pattern, inset) that is beyond the resolutions typically reached in biological applications (TEM).

3.2. Vitrified samples

For test purposes we have used two well-characterized biomolecular samples, namely 26S and 20S proteasomes. The 26S proteasome is a particularly fragile macromolecular complex of 2.5 MDa that is notoriously difficult to maintain fully intact during sample preparation (Nickell et al., 2009). Its purification involves sucrose density gradient centrifugation; since the presence of sucrose tends to degrade the quality of the ice, repeated washing is necessary to remove most of the sucrose. As a consequence of washing, the thin aqueous film spanning the holes becomes depleted of particles while these tend to accumulate on the surrounding carbon film. Obviously the sparsity of particles in the hole-spanning re-

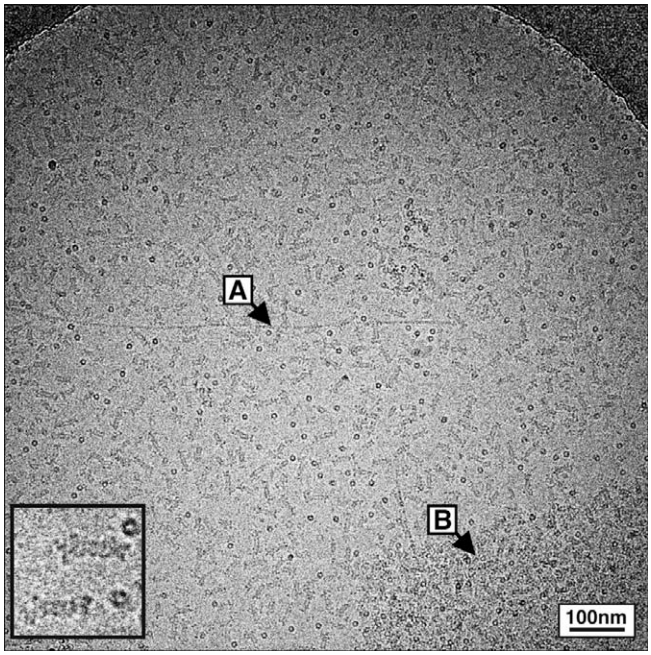

Fig. 4. Vitrified 26S proteasome prepared on graphene oxide: The 26S proteasome vitrified with a graphene oxide substrate to improve distribution (88,500× magnification, pixel size 3.5 Å). In order to ensure clarity in print, the image has been taken far from focus (−6.5 μm) and grayscale equalized. At a nominal concentration of ~0.1 mg/ml (half of that typically used) and three washes by complete buffer exchange, there are still abundant concentrations in ice. Arrows A and B indicate a long crinkle and thicker overlapping layer on the substrate, respectively. Otherwise, there is minimal attenuation of contrast by the graphene oxide substrate. The inset features individual projections at high magnification indicating the native state of individual 26S molecules (here the main scale bar corresponds to 33 nm).

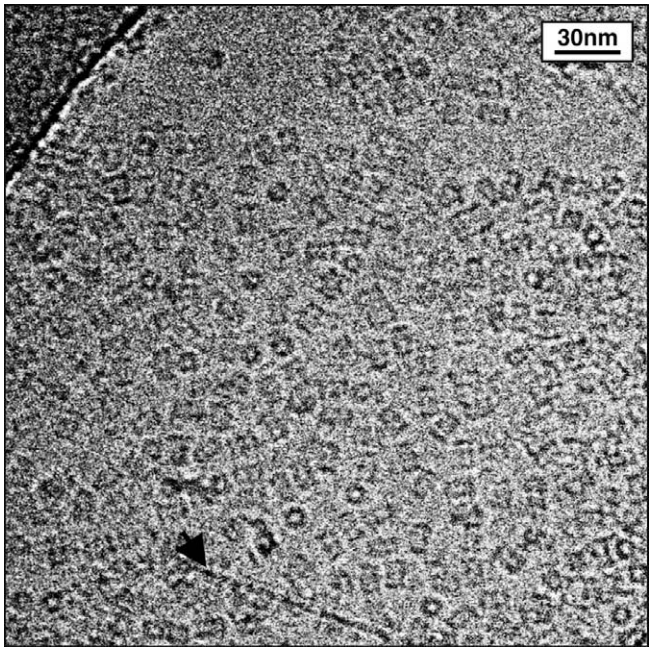

Fig. 5. Unstained 20S proteasome on graphene oxide: Fig. 4 shows unstained 20S proteasome on thin graphene oxide substrate (88,500× magnification, pixel size 3.5 Å). The image has been taken far from focus (−6.3 μm) and grayscale equalized to ensure clarity in print. The minimal contrast of the graphene oxide substrate makes it superior to standard amorphous carbon in the imaging of unstained molecules under low-dose conditions (an arrow indicates a small crinkle in the graphene oxide substrate).

gions imaged makes data collection inefficient. The presence of an additional thin graphene oxide substrate across the holes retains the particles through multiple exchanges of aqueous medium, ensuring satisfactory particle distribution (Fig. 4). In fact, the initial protein concentration (~0.1 mg/ml nominal) from the experiment documented in this figure was half that normally used with frozen-hydrated samples of 26S proteasome (~0.2 mg/ml) and yet concentration was high across the grid. The additional thin graphene oxide substrate withstands plunging forces and any attenuation of contrast is minimal; only defects such as folds, creases (Fig. 4A) or overlaps (Fig. 4B) indicate that there is an additional substrate.

The presence of a graphene oxide substrate facilitates more extensive blotting of the aqueous film than would be possible without a solid substrate, resulting in thinner ice films. In the case of the 20S proteasome preparation we have deliberately blotted to the extent that probably only strongly bound water remains. It is obviously essential that controlled ambient conditions be maintained such that molecules retain hydration in order to preserve high-resolution structure. The micrograph shown in Fig. 5 taken under low-dose conditions (~20 e/Å^2) shows the 20S proteasomes with remarkable clarity and contrast.

4. Discussion

The advantages of very thin crystalline sheets prepared of materials such as graphite or layered silicates for the electron microscopy of small single particles has been recognized long ago (Hahn and Baumeister, 1974; Dobelle and Beer, 1968). They are highly transparent and essentially featureless at resolutions below the intrinsic material periodicity, and if necessary the periodic signal can be subtracted (Meyer et al., 2008). Nevertheless, practical applications as specimen supports have been very few. Exfoliation and deposition methods are complicated and difficult to perform in a controlled manner and the inert surface properties of graphite (i.e. hydrophobicity) for example, initially proved problematic in depositing biological materials. Moreover, with the pervasive use of image averaging techniques the signal-to-noise ratio of the primary images had become less important.

Recently, developments in the fabrication of graphene have renewed interest in such specimen supports for electron microscopy (Wilson et al., 2009). The 0.34 nm thin graphene sheets are highly transparent and stable under an electron beam at relatively high doses (10^5 e$^-$/Å^2 at 300 keV) well outside those applied to biological samples. In addition to these properties, the remarkable electronic and mechanical properties of graphene make it a promising imaging substrate for electron microscopy (Chen et al., 2008; Ziegler, 2006; Zakharchenko et al., 2009; Wang et al., 2009). Untreated 'pristine' graphene is inert and so biological macromolecules do not readily adhere when applied from solution. Nevertheless, we could envisage some interesting applications of the 'ultimate preparative substrate' when molecules are deposited from the gas phase, for example in mass spectrometry (Benesch et al., 2009). Relatively small, unstained molecules will also clearly gain in contrast and SNR given the minimal background signal of graphene.

Graphene oxide is a 'functionalized' derivative of graphene to which biological samples readily attach. Due to the presence of covalently bound functional groups, graphene oxide is on average slightly thicker than pristine graphene (~1 nm Wang et al., 2009; Stankovich et al., 2006) and does demonstrate, however minimal scattering and background. The oxidization of the material also attenuates the conductivity of graphene, where oxidized regions act locally as an insulator (Gomez-Navarro et al., 2007). However, after partial reduction by baking at ~200 °C, the removal of water

and labile oxygen groups partially restores conductivity to a degree significantly higher than that of amorphous carbon, also at liquid nitrogen temperatures (Jung et al., 2008; Dawson and Adkins, 1995; Robertson, 1986). As functionalization introduces minor defects to the crystalline structure from which graphene derives its mechanical properties, a reduction in mechanical strength and elasticity is to be expected. However, substrates are stable and withstand strong plunging forces (note also the use of sonication to exfoliate sheets). Regardless, the significant reduction in background signal over amorphous carbon alone (Fig. 2) is highly desirable and should clearly improve the contrast of small molecules bound to substrate. The simplicity by which thin graphene oxide substrates covering anywhere upwards of 70–80% of the grid also ensures this method is highly accessible.

We have explored the use of graphene oxide as a substrate for the imaging of frozen-hydrated biomolecular samples. Substrates demonstrate the retained binding of the 26S proteasome (Fig. 4) such that even after repeated exchanges of buffer solution, particle density is highly satisfactory. Moreover, the attachment of particles to the graphene oxide substrate appears to stabilize this fragile complex such that the majority of particles remain intact. Hence, graphene oxide performs the same function as additional amorphous carbon substrate, however, with the benefit of significantly reduced background.

A variant of the method explored here with the 20S proteasome is to perform exhaustive blotting, removing as much buffer as possible prior to plunge freezing (Fig. 5). This would not be possible if a self-supporting vitreous ice film was to be formed. We assume that under the conditions of this experiment (performed in a controlled humidity) only bound water retained by the molecules remains rather than a continuous vitreous ice film. This is important in maintaining structural integrity of the sample and by carefully regulating the removal of excess water the contrast of individual molecules should be further optimized.

Acknowledgments

This work was supported by the European Union within the 7th Framework Programme of "PROSPECTS" and by the DFG Cluster of Excellence: Munich-Centre for Advanced Photonics (MAP). We thank Ravi Shankar Sundaraman and Marko Burghardt (MPI for solid state research, Stuttgart, Germany) for the initial graphite oxide preparations and instructions on preparation. Protein preparations of 26S and 20S proteasome were kindly provided by Oana Mihalache and Susanne Witt (MPI of Biochemistry, Martinsried, Germany). For providing access to their in-house Titan TEM we thank FEI Nanoport (Eindhoven, The Netherlands) as well as Jörg Jinschek, Christoph Mitterbauer and Gijs Van Duinen for their generous assistance.

References

Benesch, L.P., Ruotolo, B.T., Simmons, D.A., Barrera, N.P., Morgner, N., Wang, L., Saibil, H.R., Robinson, C.V., 2009. Visualizing protein assemblies by means of preparative mass spectrometry and microscopy. J. Struct. Biol. (submitted for publication).

Chen, J.H., Jang, C., Adam, S., Fuhrer, M.S., Williams, E.D., Ishigami, M., 2008. Charged-impurity scattering in graphene. Nat. Phys. 4, 377–381.

Dawson, J.C., Adkins, C.J., 1995. Conduction mechanisms in amorphous carbon prepared by ion-beam sputtering. J. Phys. Cond. Matter 7, 6297–6315.

Dobelle, W.H., Beer, M., 1968. Chemically cleaved graphite support films for electron microscopy. J. Cell Biol. 39, 733–735.

Eda, G., Fanchini, G., Chhowalla, M., 2008. Large-area ultrathin films of reduced graphene oxide as a transparent and flexible electronic material. Nat. Nanotech. 3, 270–274.

Geim, A.K., Novoselov, K.S., 2007. The rise of graphene. Nat. Mater. 6, 183–191.

Gomez-Navarro, C., Weitz, R.T., Bittner, A.M., Scolari, M., Mews, A., Burghard, M., Kern, K., 2007. Electronic transport properties of individual chemically reduced graphene oxide sheets. Nano Lett. 7, 3499–3503.

Hahn, M., Baumeister, W., 1974. High resolution negative staining of ferritin molecules on vermiculite single crystal supports. Biochim. Biophys. Acta 371, 267.

Hummers Jr., W.S., Offeman, Richard E., 1958. Preparation of graphitic oxide. J. Am. Chem. Soc. 80, 1339.

Jung, I., Dikin, D.A., Piner, R.D., Ruoff, R.S., 2008. Tunable electrical conductivity of individual graphene oxide sheets reduced at "low" temperatures. Nano Lett. 8, 4283–4287.

Lee, C., Wei, X., Kysar, J.W., Hone, J., 2008. Measurement of the elastic properties and intrinsic strength of monolayer graphene. Science 321, 385.

Lerf, A., He, H., Forster, M., Klinowski, J., 1998. Structure of graphite oxide revisited. J. Phys. Chem. B 102, 4477–4482.

Meyer, J.C., Geim, A.K., Katsnelson, M.I., Novoselov, K.S., Booth, T.J., Roth, S., 2007. The structure of suspended graphene sheets. Nature 446, 60–63.

Meyer, J.C., Girit, C.O., Crommie, M.F., Zettl, A., 2008. Hydrocarbon lithography on graphene membranes. Appl. Phys. Lett. 92, 123110.

Meyer, J.C., Girit, C.O., Crommie, M.F., Zettl, A., 2008. Imaging and dynamics of light atoms and molecules on graphene. Nature 454, 319–322.

Nickell, S., Beck, F., Korinek, A., Mihalache, O., Baumeister, W., Plitzko, J.M., 2007. Automated cryoelectron microscopy of single particles applied to the 26S proteasome. FEBS Lett. 581, 2751–2756.

Nickell, S., Beck, F., Scheres, S.H.W., Korinek, A., Forster, F., Lasker, K., Mihalache, O., Sun, N., Nagya, I., Sali, A., Plitzko, J.M., Carazo, J.M., Mann, M., Baumeister, W., 2009. Insights into the molecular architecture of the 26S proteasome. PNAS – US 106, 11943–11947.

Paredes, J.I., Villar-Rodil, S., Martinez-Alonso, A., Tascon, J.M.D., 2008. Graphene oxide dispersions in organic solvents. Langmuir 24, 10560–10564.

Reina, A., Jia, X.T., Ho, J., Nezich, D., Son, H.B., Bulovic, V., Dresselhaus, M.S., Kong, J., 2009. Large area, few-layer graphene films on arbitrary substrates by chemical vapor deposition. Nano Lett. 9, 30–35.

Robertson, J., 1986. Amorphous carbon. Adv. Phys. 35, 317–374.

Schniepp, H.C., Li, J.L., McAllister, M.J., Sai, H., Herrera-Alonso, M., Adamson, D.H., Prud'homme, R.K., Car, R., Saville, D.A., Aksay, I.A., 2006. Functionalized single graphene sheets derived from splitting graphite oxide. J. Phys. Chem. – US B 110, 8535–8539.

Stankovich, S., Dikin, D.A., Dommett, G.H.B., Kohlhaas, K.M., Zimney, E.J., Stach, E.A., Piner, R.D., Nguyen, S.B.T., Ruoff, R.S., 2006. Graphene-based composite materials. Nature 442, 282–286.

Wang, G.X., Wang, B., Park, J., Yang, J., Shen, X.P., Yao, J., 2009. Synthesis of enhanced hydrophilic and hydrophobic graphene oxide nanosheets by a solvothermal method. Carbon 47, 68–72.

Wang, G.X., Shen, X.P., Wang, B., Yao, J., Park, J., 2009. Synthesis and characterisation of hydrophilic and organophilic graphene nanosheets. Carbon 47, 1359–1364.

Wei, Z.Q., Barlow, D.E., Sheehan, P.E., 2008. The assembly of single-layer graphene oxide and graphene using molecular templates. Nano Lett. 8, 3141–3145.

Wilson, N.R., Pandey, P.A., Beanland, R., Young, R.J., Kinloch, I.A., Gong, L., Liu, Z., Suenaga, K., Rourke, J.P., York, S.J., Sloan, J., 2009. Graphene oxide: structural analysis and application as a highly transparent support for electron microscopy. ACS Nano 3, 2547–2556.

Zakharchenko, K.V., Katsnelson, M.I., Fasolino, A., 2009. Finite temperature lattice properties of graphene beyond the quasiharmonic approximation. Phys. Rev. Lett. 102, 046808.

Zhang, X.Y., Huang, Y., Wang, Y., Ma, Y.F., Liu, Z.F., Chen, Y.S., 2009. Synthesis and characterization of a graphene-C-60 hybrid material. Carbon 47, 334–337.

Ziegler, K., 2006. Robust transport properties in graphene. Phys. Rev. Lett. 97, 266802.

Zwickl, P., Lottspeich, F., Baumeister, W., 1992. Expression of functional *Thermoplasma acidophilum* proteasomes in *Escherichia coli*. FEBS Lett. 312, 157.